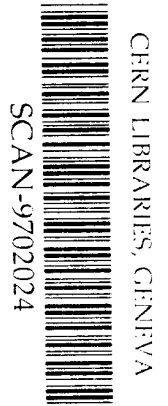# ERNEST ORLANDO LAWRENCE
BERKELEY NATIONAL LABORATORY

Supersymmetry at LHC

A. Bartl, J. Söderqvist, F. Paige, L. Poggioli,
H. Baer, R. Cahn, I. Hinchliffe, M. Shapiro, W. Yao,
C.-H. Chen, A. Seiden, J. Pilcher, X. Tata, A. Skuja,
W.B. Campbell, and A. White
Physics Division

SCAN-9702024

CERN LIBRARIES, GENEVA

DISCLAIMER

Supersymmetry at LHC

A. Bartl
University of Vienna, Vienna, Austria

J. Söderqvist
Royal Institute of Technology (KTH), Stockholm, Sweden

F. Paige
Brookhaven National Laboratory, Upton, New York

L. Poggioli
CERN, Geneva, Switzerland

H. Baer
Florida State University, Tallahasse, Florida

R. Cahn, I. Hinchliffe, M. Shapiro, and W. Yao
Ernest Orlando Lawrence Berkeley National Laboratory,
University of California, Berkeley, California 94720

C.-H. Chen
University of California, Davis, California

A. Seiden
University of California, Santa Cruz, California

J. Pilcher
University of Chicago, Chicago, Illinois

X. Tata
University of Hawaii, Honolulu, Hawaii

A. Skuja
University of Maryland, College Park, Maryland

W.B. Campbell
University of Nebraska, Lincoln, Nebraska

A. White
University of Texas, Arlington, Texas

November 1996

Supersymmetry at LHC

A. Bartl
University of Vienna, Vienna, Austria
J. Söderqvist
Royal Institute of Technology (KTH), Stockholm, Sweden
F. Paige
Brookhaven National Laboratory, Upton, NY
L. Poggioli
CERN, Geneva, Switzerland
H. Baer
Florida State University, Tallahasse, FL
R. Cahn, I. Hinchliffe, M. Shapiro, W. Yao
Lawrence Berkeley National Laboratory, Berkeley, CA
C.-H. Chen
University of California, Davis, CA
A. Seiden
University of California, Santa Cruz, CA
J. Pilcher
University of Chicago, Chicago, IL
X. Tata
University of Hawaii, Honolulu, HI
A. Skuja
University of Maryland, College Park, MD
W. B. Campbell
University of Nebraska, Lincoln, NE
A. White
University of Texas, Arlington, TX

ABSTRACT

We have developed a strategy for the analysis of experimental data at LHC which will allow us to determine the scale for supersymmetry, to limit the model parameter space, and to make precision measurements of model parameters.

I. INTRODUCTION

Supersymmetry (SUSY) is an appealing concept which provides a plausible solution to the "fine tuning" problem, while leaving the phenomenological success of the Standard Model (SM) unchanged [1]. Moreover, some SUSY models allow for the unification of gauge couplings at a scale of $M_{GUT} \approx 10^{16}$ GeV. A further attractive feature is the possibility of radiative breaking of the electro-weak symmetry group $SU(2) \times U(1)$. The masses of the SUSY partners of the SM particles are expected to be in the range 100 GeV to 1 TeV. One of the main goals of the Large Hadron Collider (LHC) will be either to discover "weak-scale" SUSY or to exclude it over the entire theoretically allowed parameter space.

Several studies in the past demonstrated that LHC is an excellent machine to search for SUSY particles [2, 3, 4, 5]. These studies were usually performed in the "Minimal Supersymmetric Standard Model (MSSM)", and they have shown that gluinos of mass less than 2 TeV and the first and second generation squarks of mass less than 1 TeV can be detected at LHC. It will also be possible to detect direct production of scalar top quarks, scalar bottom quarks, sleptons, charginos and neutralinos over a more restricted mass range. Direct production of weakly interacting particles is not the main source of these particles at LHC. They may, however, be produced in cascade decays of gluinos and squarks with sufficient rates, so their properties may be studied there. This is particularly the case in the parameter region where the lightest neutralino $\tilde{\chi}_1^0$, assumed to be the lightest SUSY particle (LSP), is a good candidate for dark matter [6].

Determining SUSY masses will be difficult, however, because each SUSY event contains two LSP's, and there are not enough kinematic constraints to determine their momenta. Many signals will have a background from SM reactions which in some cases can be quite large, and which has to be subtracted. Furthermore, all SUSY particles which are kinematically accessible

will be simultaneously produced, and their contributions to the SUSY signals must be disentangled. Generally, when analysing a particular SUSY reaction, the background will mainly come from the other SUSY channels. This point will be particularly important for precision measurements of SUSY parameters.

All SUSY particle masses, production cross sections and decay branching ratios, are model dependent. Vice versa, measuring the distributions of characteristic variables will provide valuable information on SUSY model parameters.

The range of possible SUSY signatures at LHC has been discussed extensively in the literature [4]. We take the SUSY analysis one step further and discuss how to measure SUSY particle masses and branching ratios, and how these measurements then relate to SUSY models. Specifically in this report the following questions are addressed:

(i) Once a SUSY signal is observed at LHC, how can experiments differentiate between models?

(ii) Can models be ruled out by showing them to be inconsistent with data?

(iii) Can the parameters of candidate models be constrained?

We report on a strategy we have developed which allows us to answer these questions in a definite way. The strategy enables us to extract the characteristic experimental quantities as, for example, masses and branching ratios. This allows us to determine the relevant parameters.

First we identify the LHC experimental detector capabilities. Then we present case studies where we use the five different parameter sets recently selected for SUSY studies at LHC. From these case studies we develop the strategy for the general analysis of the experimental data. The strategy varies with the SUSY parameters, or which SUSY model is being tested. We then give some examples which will indicate the general level of precision available at LHC in SUSY studies.

II. EXPERIMENTAL CONDITIONS

The LHC is a pp collider with an energy of $\sqrt{s} = 14$ TeV in the center of mass. LHC is planned to be commissioned in the year 2005. Data will be taken first at "low" luminosity for a few years ($\mathcal{L} \approx 10^{33} cm^{-2} s^{-1}$), and then at "high" luminosity ($\mathcal{L} \approx 10^{34} cm^{-2} s^{-1}$). An integrated luminosity of 10^4 pb^{-1} (10^5 pb^{-1}) per year is expected for low (high) luminosity.

There will be two general purpose experiments, ATLAS [2] and CMS [3]. They are designed to discover "new physics" phenomena at high transverse momentum. Both detectors will have:

(i) A precision electromagnetic calorimeter (as dictated e. g. by the search for the $h \rightarrow \gamma\gamma$ mode), typical energy resolution of 10 %/$\sqrt{E} \oplus 1$ %

(ii) Good lepton (e, μ) identification for rapidity $|\eta| < 3$, with an efficiency $\geq$ 90 %

(iii) A calorimeter system for reconstructing jets and measuring their momentum

(iv) a hadron calorimeter with coverage up to $|\eta| \approx 5$ which allows for good measurement of missing transverse energy, for ATLAS the resolution is expected to be $0.46\sqrt{\Sigma E_T}$ for low luminosity [2]

(v) multilayer silicon and pixel detectors which will allow heavy flavor tagging, with efficiency $\epsilon_b \geq 60\%$ and mistagging of < 10%(< 1%) for c-jets (light jets) at low luminosity [3, 7].

There is no pile-up of minimum bias events, that effects the performance at low luminosity. In this report only low luminosity is simulated and results are quoted for one year of data-taking if not explicitly stated differently. At high luminosity the tracking system is degraded and the b-tagging efficiency is reduced.

III. THEORETICAL FRAMEWORK

In our study we have considered only the "minimal supergravity model" which we describe below. On the one hand, this model has only five parameters and provides a well defined theoretical framework for the calculation of SUSY particle masses, production cross sections, decay branching ratios etc. On the other hand, it is flexible enough to study a large variety of different SUSY signals [8]. Many of the methods described here should be applicable to other models, provided R-parity is conserved. Of course, as the model is made more general, it becomes more difficult to determine all parameters.

A. The minimal supergravity model

We performed our analysis in the framework of the "minimal supergravity-inspired model", in the following abbreviated by "mSUGRA" (often also called "constrained MSSM"). In this class of models the weak, electromagnetic and strong coupling parameters α_i, $i = 1, 2, 3$, unify at the scale $M_{GUT} \approx 10^{16}$ GeV, and electroweak symmetry is radiatively broken. Furthermore, the three gaugino masses M_i, the scalar masses m_i, and the trilinear coupling parameters A_{ijk} are also unified at a high scale which in mSUGRA is assumed to be M_{GUT}. Even within this restricted framework there is a wide range of models. These are characterized by a set of five parameters m_0, $m_{1/2}$, A_0, $\tan\beta$, and $sgn(\mu)$. The soft-breaking parameters m_0, $m_{1/2}$, and A_0, are the common scalar mass, the common gaugino mass, and the common trilinear scalar coupling constant, respectively, at M_{GUT}. Also $\tan\beta$ is the ratio of the vacuum expectation values of the two Higgs doublets, and μ is the Higgs-higgsino mass parameter whose sign has to be chosen. Giving up the assumption of radiative symmetry breaking would be tantamount to chosing μ^2 as a free parameter. The masses of all SUSY particles are then calculated at the weak scale with the help of renormalization group equations (RGEs). We show in Fig. 1 SUSY particle masses in a representation of the parameter space of the mSUGRA model in the m_0 vs. $m_{1/2}$ plane for $\tan\beta = 2$, $\mu > 0$ and $A_0 = 0$.

The bricked region is excluded either because electroweak symmetry is not broken appropriately, or because the lightest
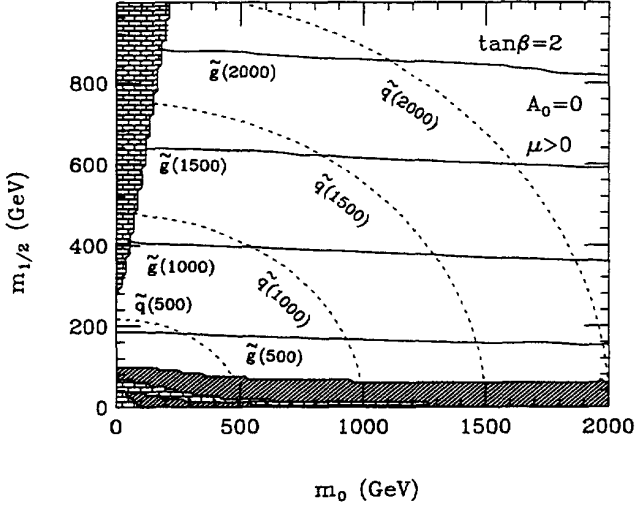
Figure 1: Sparticle masses in mSUGRA displayed in the m_0 vs. $m_{1/2}$ plane for $\tan\beta = 2$, $\mu > 0$ and $A_0 = 0$.

Table I: Effect on 3rd generation scalar quarks due to A_0.

A_0 (GeV)	$m_{\tilde{t}_1}$ (GeV)	$m_{\tilde{b}_1}$ (GeV)	BR($\tilde{g} \to \tilde{b}_1 b$) %
-400	234	278	88.7
0	264	266	94.2
500	269	272	89.5

for stops, and analogous ones for sbottoms and staus, where the the off-diagonal term is $m_{b,\tau}(A_{b,\tau} - \mu\tan\beta)$ Because of these two effects the lower mass eigenvalues of stop, sbottom, and stau can be considerably smaller than the masses of the sfermions of the 1st and 2nd generation.

Charginos and neutralinos, are in general, mixtures of gauginos and higgsinos, where the mixing depends on the SUSY parameters. At the weak scale, the neutralino and chargino masses are approximately

$$m_{\tilde\chi_1^0} \approx 0.4m_{1/2}, \quad m_{\tilde\chi_2^0} \approx m_{\tilde\chi_1^\pm} \approx 0.8m_{1/2},$$

and

$$m_{\tilde\chi_3^0} \approx m_{\tilde\chi_4^0} \approx m_{\tilde\chi_2^\pm} \approx |\mu|,$$

where in mSUGRA typically $|\mu| \gg m_{1/2}$, although exceptions are possible in some regions of parameter space. The numerical value of $|\mu|$ is determined by the condition of radiative symmetry breaking and depends on the mSUGRA parameters. As a rule, the dominant component of $\tilde\chi_1^0$ is $\tilde{B}$, the dominant components of $\tilde\chi_2^0$ and $\tilde\chi_1^\pm$ are $\widetilde{W}^3$ and $\widetilde{W}^\pm$, whereas $\tilde\chi_3^0$, $\tilde\chi_4^0$, and $\tilde\chi_2^\pm$ are mainly higgsinos. However, there may be an appreciable admixture of the other components. The amount of admixture of the subdominant components is roughly of the order of $m_Z/m_{1/2}$ or m_Z/μ.

The gluino mass is roughly given by

$$m_{\tilde{g}} \approx 2.4m_{1/2},$$

however, corrections to this formula up to 30% are possible.

The parameter A_0 only plays a role in the sector of the sfermions of the 3rd generation. However, even here its influence is rather weak in most of the examples studied. The reason is that at the weak scale the parameters A_t and A_b very often turn out to be near their fixed–point value $-2.1m_{1/2}$. Our results, therefore, do not strongly depend on the numerical value of A_0. As an example we take the parameter set D of Table II (see Subsection B below) and vary A_0 between -400 GeV and 500 GeV. We show in Table I the masses of $\tilde{t}_1$ and $\tilde{b}_1$, the lighter eigenstates of the 3rd generation scalar quarks, and the branching ratio for the decay $\tilde{g} \to \tilde{b}_1 b$. As can be seen, these results are relatively insensitive to A_0.

B. Choice of Parameters

The ATLAS and CMS Collaborations at LHC are considering five points in the mSUGRA model for their analyses. The

neutralino is not the LSP. The shaded region is excluded by experimental searches for SUSY at LEP and TEVATRON experiments. We show contours of $m_{\tilde{q}}$ and $m_{\tilde{g}}$ here to be compared with LHC reach plots for mSUGRA (see Fig. 3). The model is described in more detail in the report of the SUSY Theory Subgroup in these Proceedings [8].

For our analysis we use the form of the RGEs as implemented in ISAJET [9]. The masses of squarks and sleptons of the 1st and 2nd generation are given by

$$m_{\tilde{f}_{L,R}}^2 = m_0^2 + m_f^2 + c(\tilde{f}_{L,R}) \cdot m_{1/2}^2 + D(\tilde{f}_{L,R}),$$

with the coefficient

$$c(\tilde{f}_L) \approx 6 \text{ for } \tilde{f}_L = \tilde{u}_L, \tilde{d}_L,$$

$$c(\tilde{f}_R) \approx 5.5 \text{ for } \tilde{f}_R = \tilde{u}_R, \tilde{d}_R,$$

$$c(\tilde{f}_L) \approx 0.5 \text{ for } \tilde{f}_L = \tilde{\ell}_L, \tilde{\nu}_\ell,$$

$$c(\tilde{f}_R) \approx 0.15 \text{ for } \tilde{f}_R = \tilde{e}_R,$$

and with the D-term

$$D(\tilde{f}_{L,R}) = \pm(T_f^3 - Q_f \sin^2\Theta_W)m_Z^2\cos 2\beta$$

For the sfermions of the 3rd generation the Yukawa interactions reduce the soft SUSY breaking masses of the left- and right sfermions, and also induce a mixing which is described by a 2×2 mass matrix

$$\begin{pmatrix} m_{\tilde{f}_L}^2 & m_t(A_t - \mu\cot\beta) \\ m_t(A_t - \mu\cot\beta) & m_{\tilde{f}_R}^2 \end{pmatrix}$$

3

Table II: SUGRA parameters for the five LHC points

Point	m_0 (GeV)	$m_{1/2}$ (GeV)	A_0 (GeV)	$\tan\beta$	sgn μ
A	100	300	300	2.1	+
B	400	400	0	2.0	+
C	400	400	0	10.0	+
D	200	100	0	2.0	−
E	800	200	0	10.0	+

Table III: Masses of SUSY particles in GeV for the five LHC points

Point	A	B	C	D	E
$\tilde{g}$	767	1004	1009	298	582
$\tilde{\chi}_1^{\pm}$	232	325	321	96	147
$\tilde{\chi}_2^{\pm}$	518	764	537	272	315
$\tilde{\chi}_1^0$	122	168	168	45	80
$\tilde{\chi}_2^0$	233	326	321	97	148
$\tilde{\chi}_3^0$	497	750	519	257	290
$\tilde{\chi}_4^0$	521	766	538	273	315
$\tilde{u}_L$	687	957	963	317	918
$\tilde{u}_R$	664	925	933	313	910
$\tilde{d}_L$	690	959	966	323	921
$\tilde{d}_R$	662	921	930	314	910
$\tilde{t}_1$	489	643	710	264	594
$\tilde{t}_2$	717	924	933	329	805
$\tilde{b}_1$	633	854	871	278	774
$\tilde{b}_2$	663	922	930	314	903
$\tilde{e}_L$	239	490	491	216	814
$\tilde{e}_R$	157	430	431	207	805
$\tilde{\nu}_e$	230	486	485	207	810
$\tilde{\tau}_1$	157	430	425	206	797
$\tilde{\tau}_2$	239	490	491	216	811
$\tilde{\nu}_\tau$	230	486	483	207	806
h^0	104	111	125	68	117
H^0	638	1046	737	379	858
A^0	634	1044	737	371	859
$H^{\pm}$	638	1046	741	378	862

SUGRA parameters of these five points are shown in Table II. Point D is the so-called "comparison point" [1], as it is also used for SUSY studies at the proposed NLC and TEVATRON (TEV33) colliders. Here we shall take these five points as examples for developing our strategy to analyse SUSY data at LHC.

The masses of the SUSY particles predicted for each of these five LHC points are shown in Table III. In all cases studied we take $m_t = 175$ GeV for the mass of the top quark. Besides the five LHC Points we also study models with randomly chosen sets of SUSY parameters. In this case we assume that the mass of the Higgs particle h^0 is known within a band of ± 3 GeV. This is a conservative estimate of the theoretical error of the mass of h^0 expected at the time when LHC will operate. We restrict the range of the common scalar mass parameter and of the common gaugino mass parameter to $m_0 \leq 800$ GeV and $m_{1/2} \leq 500$ GeV. These upper bounds for m_0 and $m_{1/2}$ follow from "naturalness" arguments [10, 11]. In the analysis of [11] upper bounds for the masses of squarks and gluinos of 700 GeV and 800 GeV are obtained, while the "most natural" value for these masses is quoted to be 250 GeV. Furthermore, we restrict the range of the trilinear scalar coupling parameter to $-m_0 \leq A_0 \leq m_0$. This restriction on A_0 is more conservative than those which in general follow from the requirement that charge and color breaking minima have to be avoided.

C. Simulation

For the event simulation of the various SUSY signals and the SM background reactions the Monte Carlo ISAJET, version 7.20 [9] is used. This program contains the RGEs, and calculates all SUSY masses, production cross sections, decay rates etc. The detector response is simulated with a toy calorimeter having hadronic and electromagnetic resolution smearing, and b-tagging, lepton efficiencies etc are all included. The toy detector is tuned to the expected ATLAS and CMS performance. For the present purpose this is sufficient.

IV. SUSY PRODUCTION AND SIGNATURES

At LHC pair production of strongly interacting particles like $\tilde{g}\tilde{g}$, $\tilde{g}\tilde{q}$, and $\tilde{q}\tilde{q}$ has the largest cross section. We show in Fig. 2

[1] Point 3 for NLC and Point 2 for TEVATRON

the sum of the total cross sections of $\tilde{g}\tilde{g}$, $\tilde{g}\tilde{q}$ and $\tilde{q}\tilde{q}$ production at $\sqrt{s} = 14$ TeV, as a function of $m_{\tilde{g}}$, for $\tan\beta = 2$, $\mu = m_{\tilde{g}}$, for the two cases $m_{\tilde{q}} = m_{\tilde{g}}$ and $m_{\tilde{q}} = 2m_{\tilde{g}}$. We also show in Fig. 2 the cross section for associated production of $\tilde{g}/\tilde{q}$ with $\tilde{\chi}_i^{\pm}/\tilde{\chi}_i^0$, and for $\tilde{\chi}_1^+\tilde{\chi}_1^-$ and $\tilde{\chi}_1^+\tilde{\chi}_2^0$ production. Pair production of sleptons, charginos and neutralinos leads to very clean dilepton and trilepton events with detectable rates if the masses are smaller than about $200 - 250$ GeV [12, 13, 14]. The cross section for $\tilde{t}_1\tilde{t}_1$ production varies from about 8 pb for $m_{\tilde{t}_1} = 300$ GeV to about 80 fb for $m_{\tilde{t}_1} = 700$ GeV [15]. We give in Table IV the total cross sections for pair production of SUSY particles at the five LHC points.

Squarks and gluinos can have strong decays

$$\tilde{q}_{L,R} \rightarrow q\tilde{g},$$
$$\tilde{g} \rightarrow \bar{\tilde{q}}_{L,R}, \; \bar{q}\tilde{q}_{L,R}$$

or weak decays

$$\tilde{q}_{L,R} \rightarrow q\tilde{\chi}_i^0,$$
$$\tilde{q}_L \rightarrow q'\tilde{\chi}_i^{\pm},$$
$$\tilde{g} \rightarrow q\bar{q}\tilde{\chi}_i^0,$$
$$q\bar{q}'\tilde{\chi}_i^{\pm},$$
$$g\tilde{\chi}_i^0,$$

4

Table IV: Cross sections in fb for production of SUSY particles at the five LHC points

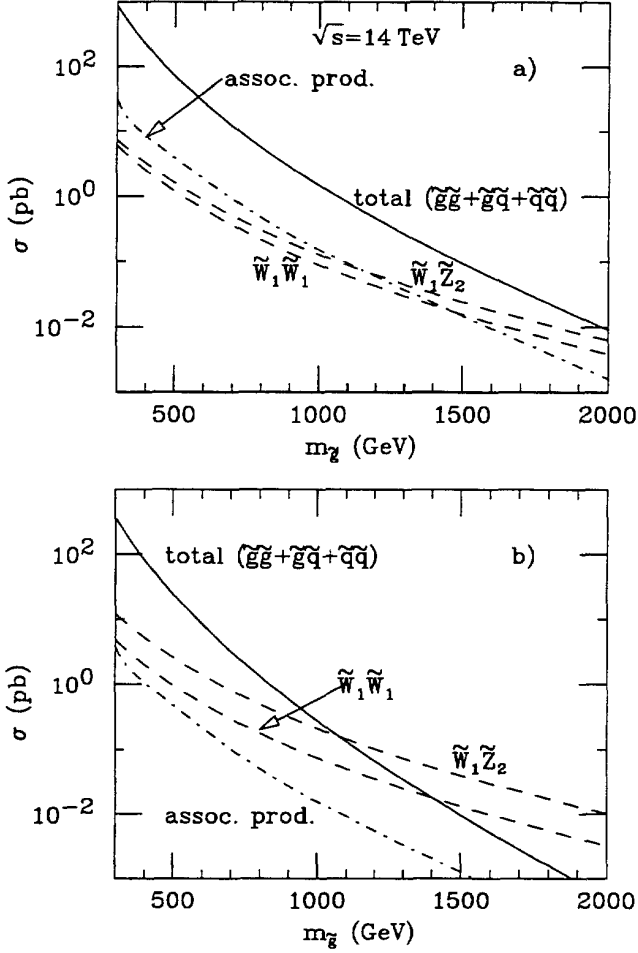| Point	A	B	C	D	E
$\tilde{g}\tilde{g}$	1751	258	259	437189	10877
$\tilde{q}\tilde{\bar{q}}$	2379	363	337	103059	455
$\tilde{q}\tilde{q}$	2820	686	672	73769	909
$\tilde{b}_i\tilde{b}_i$	297	54	34	18442	57
$\tilde{t}_i\tilde{t}_i$	701	150	95	18985	293
$\tilde{g}\,\tilde{q}^{(-)}$	8306	1486	1444	642765	8259
$\tilde{\chi}_i^{\pm}\tilde{\chi}_j^{\mp}$	242	66	75	7865	1108
$\tilde{\chi}_i^0\tilde{\chi}_j^0$	18	6	16	814	110
$\tilde{\chi}_i^{\pm}\tilde{\chi}_j^0$	521	138	146	13832	3532
$\tilde{l}_i\tilde{l}_i, \tilde{\nu}_i\tilde{\nu}_i$	253	9	13	542	—

Figure 2: SUSY production cross sections at LHC for MSSM, a) is for $m_{\tilde{q}} = m_{\tilde{g}}$, $\tan\beta = 2$, $\mu = m_{\tilde{g}}$, and b) is for $m_{\tilde{q}} = 2m_{\tilde{g}}$, $\tan\beta = 2$, $\mu = m_{\tilde{g}}$ ($\tilde{W}_i = \tilde{\chi}_i^{\pm}$ and $\tilde{Z}_j = \tilde{\chi}_j^0$).

where the strong decays are dominant if they are kinematically allowed. If the lighter stop eigenstate $\tilde{t}_1$ is the lightest visible SUSY particle, it decays into $c\tilde{\chi}_1^0$ or $bW^{\pm}\tilde{\chi}_1^0$. Otherwise both stop eigenstates decay according to

$$\tilde{t}_i \rightarrow t\tilde{\chi}_k^0,$$
$$b\tilde{\chi}_k^{\pm}.$$

If kinematically allowed, transitions such as

$$\tilde{t}_2 \rightarrow Z^0\tilde{t}_1,$$
$$h^0\tilde{t}_1,$$
$$W^{\pm}\tilde{b}_1,$$
$$H^{\pm}\tilde{b}_1$$

may also be important. Charginos and neutralinos have both leptonic and hadronic decays

$$\tilde{\chi}_i^{\pm} \rightarrow \ell^{\pm}\nu_{\ell}\tilde{\chi}_k^0,$$

$$q\bar{q}'\tilde{\chi}_k^0,$$
$$\ell^{\pm}\ell^{\mp}\tilde{\chi}_1^{\pm},$$
$$\nu_{\ell}\bar{\nu}_{\ell}\tilde{\chi}_1^{\pm},$$
$$q\bar{q}\tilde{\chi}_1^{\pm}$$

and

$$\tilde{\chi}_i^0 \rightarrow \ell^{\pm}\ell^{\mp}\tilde{\chi}_k^0,$$
$$\nu_{\ell}\bar{\nu}_{\ell}\tilde{\chi}_k^0,$$
$$q\bar{q}'\tilde{\chi}_k^0,$$
$$\ell^{\pm}\nu_{\ell}\tilde{\chi}_k^{\mp},$$
$$q\bar{q}'\tilde{\chi}_k^{\pm},$$
$$\gamma\tilde{\chi}_i^0,$$

via (virtual or real) $W^{\pm}$, Z^0, $\tilde{l}$, $\tilde{\nu}_l$, $\tilde{q}$ or Higgs particles. The cascade decays terminate when the $\tilde{\chi}_1^0$, assumed to be the LSP, is reached. If the decay into a real h^0 is kinematically possible, e.g. $\tilde{\chi}_i^0 \rightarrow h^0\tilde{\chi}_k^0$, the leptonic decay rate is reduced, while the number of b jets in the event is enhanced. For a large part of the parameter space most of the electroweakly interacting SUSY particles come from cascade decays rather than direct production. If R-parity is conserved, the $\tilde{\chi}_1^0$ is stable and provides cold dark matter. To avoid overclosing the universe, it is generally necessary to have fairly light sleptons, so that slepton exchange can cause enough of the $\tilde{\chi}_1^0$'s to annihilate [6]. These light sleptons may then contribute to chargino and neutralino decays.

As a rule, in the mass range covered by LHC, cascade decays of SUSY particles are more likely than direct transitions into the LSP [16]. The gluinos and squarks in particular can have large branching ratios for decays into charginos and higher neutralinos, which themselves may then decay in several steps.

Within the MSSM, where R-parity is conserved, SUSY events have the following characteristic signatures:
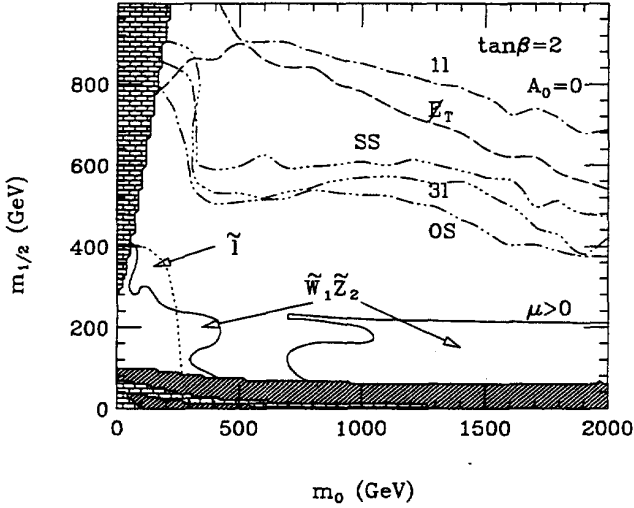
(i) large missing transverse energy $\not{E}_T$,

5

Figure 3: LHC discovery limit from 1-lepton, same-sign dilepton, opposite-sign dilepton, and 3-lepton signals displayed in the m_0-$m_{1/2}$ plane for $\tan\beta = 2$, $\text{sgn}(\mu) > 0$ and $A_0 = 0$ for one year at low luminosity ($\widetilde{W}_i = \tilde{\chi}_i^\pm$ and $\widetilde{Z}_j = \tilde{\chi}_j^0$).

Figure 4: LHC discovery limit from 1-lepton, same-sign dilepton, opposite-sign dilepton, and 3-lepton signals in R-violated mSUGRA model ($\widetilde{W}_i = \tilde{\chi}_i^\pm$ and $\widetilde{Z}_j = \tilde{\chi}_j^0$).

(ii) high multiplicity of jets with large transverse momentum p_T,

(iii) isolated leptons, and

(iv) copious production of central b jets.

Both the ATLAS and the CMS detectors at LHC are designed to clearly identify and analyse events which exhibit one or more of these characteristic features. An experimental signal for SUSY will show an excess of these events compared to the SM prediction.

V. DISCOVERY LIMITS

Several studies which were carried out in the past demonstrated that LHC will cover the whole mass range for strongly interacting SUSY particles relevant to weak-scale SUSY. For example, in [2] the mass reach obtained with the $\not{E}_T$ signature for gluinos with an integrated luminosity of 10^5 pb^{-1} (10^3 pb^{-1}) is $m_{\tilde{g}} < 1600(1050)$ GeV, $2300(1800)$ GeV, $3600(2600)$ GeV for $m_{\tilde{q}} = 2m_{\tilde{g}}$, $m_{\tilde{q}} = m_{\tilde{g}}$, $m_{\tilde{q}} = \frac{1}{2}m_{\tilde{g}}$, respectively. Similarly, in [3] possible signatures in the mass range $300 \leq m_{\tilde{g},\tilde{q}} \leq 1500$ GeV for squarks and gluinos are examined. Further studies of SUSY signals at LHC within the mSUGRA are contained in [4, 17].

We show in Fig. 3 regions of the mSUGRA plane shown in Fig. 1 where various signals for mSUGRA should be visible assuming 10 fb^{-1} of integrated luminosity.

The region below the dotted contour is where clean dileptons from slepton pair production ought to be visible. The region below the solid contour is where clean trilepton signals from
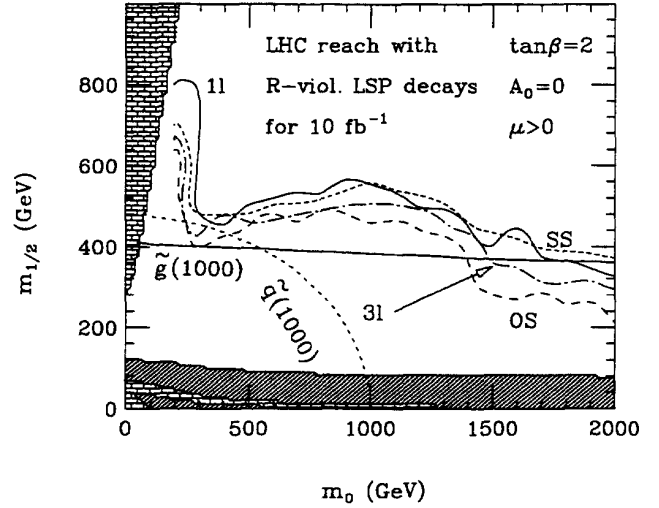
chargino/neutralino production ought to be visible. The remaining contours denote the reach in various multi-jet plus $\not{E}_T$ channels, plus 0 leptons, one lepton, two leptons (opposite-sign (OS) and same-sign (SS), and three leptons. Comparison with the mass contours from Fig. 1 shows that the greatest reach is obtained via the single lepton plus jets plus $\not{E}_T$ channel, which is approximately $m_{\tilde{g}} = 2.3$ TeV for low m_0, and $m_{\tilde{g}} = 1.7$ TeV for large m_0[4].

In SUSY models with R-parity violation, the LSP will decay, and the missing transverse energy signal is diminished. If R-parity is violated to only a small extent the LSP may decay outside the detectors, and then the signatures and the analysis do not change. If R-parity violation originates from pure lepton number violation, the LSP will decay into two leptons and a neutrino, or into two jets plus a lepton or neutrino. If the LSP decays into leptons, every SUSY event will contain several extra leptons providing an unambigous signature. If R-parity violation is due to baryon number violation the LSP will decay into 3-quark states (jets).

A calculation has been performed in Ref. [18] where additional B and R-parity violating interactions are assumed to be present in the SUSY Lagrangian, but at sufficiently small levels that ordinary gauge and Yukawa interactions still dominate the production and decay mechanisms. In this case, the sole effect of R-parity violation will be that the LSP decays into 3-quark states. In Ref. [18], it was assumed $\chi_1^0 \rightarrow cds$ or $\bar{c}\bar{d}\bar{s}$ states. Then, exactly the same cuts were applied to the search for SUSY signals as in Ref. [4] The reach of LHC in various channels is shown in Fig. 4 for the same parameters as in Fig. 3.

The reach for mSUGRA in this case in the single lepton channels (1ℓ), dilepton channels (OS and SS) and trilepton channels (3ℓ) are denoted by the various labeled contours. The reach is significantly diminished from that shown in Fig. 3. But even

6

so, there exists a sufficient number of events surviving the cuts to be able to probe beyond $m_{\tilde{g}}$ or $m_{\tilde{q}}$ values as high as 1 TeV, with just $10\mathrm{fb}^{-1}$ of integrated luminosity. Thus, if the fine-tuning bounds from [10, 11] are taken seriously, even in this difficult case R-parity violating mSUGRA should be detectable at LHC. In this case, the gluino and squark cascade decays deliver enough leptons and neutrinos to allow a broad range of parameter space to be explored by experiments using cuts designed for R-parity conserving SUSY. The $\not{E}_T$ signal is, of course, not useful in this scenario; instead the additional jet-multiplicity may be used as a SUSY signature. If cuts are designed to search explicitly for R-parity violating SUSY, then the SUSY reach will certainly be greater than that shown in Fig. 4.

VI.   STRATEGY FOR DETERMINING SUSY PARAMETERS

In order to prove that an observed deviation from the SM originates from SUSY, and to measure the underlying SUSY parameters, we propose the following strategy:

Step 1: Establish that there is an excess of events with a characteristic SUSY signature, i.e. with large $\not{E}_T$, a large number of high-p_T jets, and isolated leptons. The cross section and magnitude of the $\not{E}_T$ and of the p_T of the jets and leptons indicate the mass scale of "new physics".

Step 2: Study the distributions in some characteristic variables and show that SUSY is a candidate for the explanation.

Step 3: Test the predictions of candidate SUSY models. Determine the parameters for those models which pass this test.

The ultimate goal is to measure a sufficiently large number of characteristic distributions to perform a global fit of the data, in a similar way as is done,for example, with Z^0 data at LEP.

VII.   STEP 1: EFFECTIVE MASS ANALYSIS - DETERMINING SUSY MASS SCALE

SUSY production at LHC is dominated by the production of gluinos and squarks, which decay into multiple jets plus missing energy. The mass scale of this SUSY signal can be estimated by using the effective mass, which is defined as the scalar sum of the p_T's of the four hardest jets and the missing transverse energy $\not{E}_T$ [19]:

$$M_{\mathrm{eff}} = p_{T,1} + p_{T,2} + p_{T,3} + p_{T,4} + \not{E}_T$$

We show in Fig. 5 the M_{eff} distributions for signal and background for point A of Table II. The same distributions for the other LHC points considered in this report are shown in Ref. [19].

At high M_{eff} one can see that the SUSY signal is much larger than the SM background. The peak of the M_{eff} mass distribution, or alternatively the point at which the signal and background are equal, provides a good first estimate of the SUSY mass scale, which is defined to be
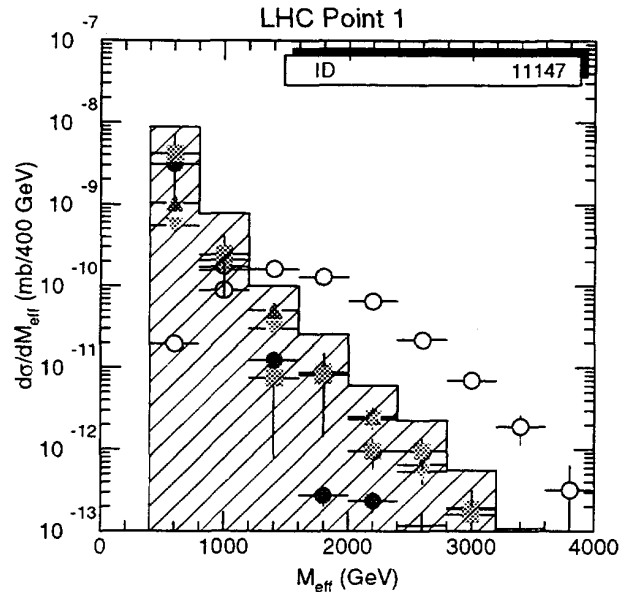
$$M_{\mathrm{SUSY}} = \min(m_{\tilde{g}}, m_{\tilde{u}_R})$$

Figure 5: Signal and SM backgrounds for Point B. Open circles: signal. Solid circles: $t\bar{t}$. Triangles: $W \to \ell\nu, \tau\nu$. Downward triangles: $Z \to \nu\bar{\nu}, \tau\tau$. Squares: QCD jets.

(The choice of $m_{\tilde{u}_R}$ as the typical quark mass is rather arbitrary.) The ratio, $M_{\mathrm{eff}}/M_{\mathrm{SUSY}}$, for which signal equals background is 1.48 and 1.58 for Points A and D, respectively. To check the stability of this ratio, 100 mSUGRA models were chosen at random with $100 < m_0 < 500$ GeV, $100 < m_{1/2} < 500$ GeV, $-500 < A_0 < 500$ GeV, $1.8 < \tan\beta < 12$, and sgn $\mu = \pm1$. The light Higgs was assumed to be known, and all the comparison models were required to have the same light Higgs mass, 100.4 GeV, within a theoretical uncertainty taken to be ±3 GeV. Fig. 6 shows the resulting scatter plot of M_{SUSY} vs. M_{eff}. The peak in the M_{eff} distribution correlates well with the SUSY mass scale. The ratio is constant within about $\pm10\%$.

For a discussion of the determination of M_{eff} in points B, C, D, and E, and for more details refer to [19].

VIII.   STEP 2: PRECISION MEASUREMENTS AT THE COMPARISON POINT

In this section we develop a few examples of possible analysis to demonstrate the general level of precision that can be obtained at the LHC. The analysis techniques shown here can be used in a large part of the parameter space, but how powerful they will be depend on the mSUGRA parameters.

We consider analysis for the LHC-NLC-TEV33 comparison point D (in Table II). In point D the total SUSY production cross section at LHC is 1356 pb so there will be a spectacular event sample (13.5 million SUSY events per year at low luminosity)
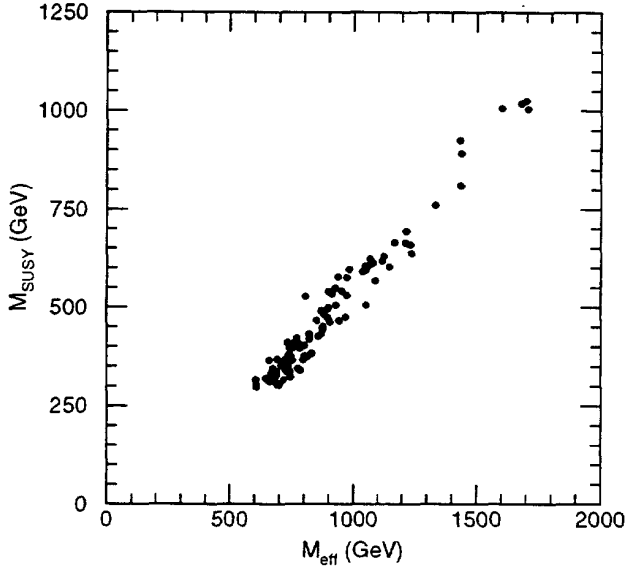
Figure 6: Scatter plot of $M_{\rm SUSY} = \min(m_{\tilde{g}}, m_{\tilde{u}})$ vs. $M_{\rm eff}$ for randomly chosen mSUGRA models having the same light Higgs mass within ± 3 GeV as that observed at Point A.

to analyse! If point D turns out to resemble the real SUSY world the light higgs boson mass is 68 GeV so it will be discovered by LEP2 before the start of the LHC experiments. The knowledge of the mass of the light higgs boson will restrict the allowed mSUGRA parameters and ease LHC analysis. However LEP2 cannot distinguish if it is a SM higgs or a SUSY higgs boson, and will not discover SUSY particles.

At point D gluino and squarks have masses around 300 GeV so dominant production modes are $(\tilde{g}\tilde{g}, \tilde{g}\tilde{q}, \tilde{q}\tilde{q})$. Gluino-pair production accounts for 32 % of the total SUSY production. The dominant decay of the gluino is

$$\tilde{g} \rightarrow \tilde{b}_L b$$
$$\quad \hookrightarrow \tilde{\chi}_2^0 b \tag{1}$$

(The notation used in the following is $\tilde{b}_{L/R}$ for the two sbottom states, for $\tan\beta = 2$ there is hardly any $\tilde{b}_L - \tilde{b}_R$ mixing, so $\tilde{b}_1 = \tilde{b}_L, \tilde{b}_2 = \tilde{b}_R$.) The branching fractions for $\tilde{\chi}_2^0$ decays are

- $BR(\tilde{\chi}_2^0 \rightarrow \tilde{\chi}_1^0 \ell^- \ell^+) = 16\ \%$ per lepton species
- $BR(\tilde{\chi}_2^0 \rightarrow \tilde{\chi}_1^0 q\bar{q})\quad = 42\ \%$

The gluino decay chain allows a powerful analysis which is described below.

If both $\tilde{\chi}_2^0$ decay leptonically in each of the LHC experiments 272 000 events per 10 fb^{-1} of integrated luminosity are produced with

- 4 b-jets
- 4 isolated leptons (2 pairs: opposite sign and same flavour)

and if one $\tilde{\chi}_2^0$ decay into leptons and the other into jets there are 694 000 events per 10 fb^{-1} of integrated luminosity with

- 4 b-jets
- 2 isolated leptons (opposite sign and same flavour)
- 2 non b-jets

From these dominant decays one can measure the mass difference between $\tilde{\chi}_2^0$ and $\tilde{\chi}_1^0$ and between $\tilde{g}$ and $\tilde{b}_L$. These two measurements have strong correlations to the global parameters of the SUSY model considered here. The evaluation of other SUSY processes will of course help to constrain candidate SUSY models further and some examples of this are also presented.

A. Measurement of the neutralino mass difference

$$m_{\tilde{\chi}_2^0} - m_{\tilde{\chi}_1^0}$$

At LHC the production and subsequent cascade decays of gluinos will result in many $\tilde{\chi}_2^0 \rightarrow \tilde{\chi}_1^0 \ell^- \ell^+$ decays. This three body decay offer a unique opportunity to get precise information on the neutralino mass difference[13]. The cuts used here to get a clean gluino cascade decay with leptonic $\tilde{\chi}_2^0$ decays are:

- ≥ 6 jets of which at least 3 are tagged as b-jets
- 2 isolated leptons of opposite sign and same flavour (e or μ)

The dilepton invariant mass is reconstructed and the resulting invariant mass spectrum is shown in Fig. 7. There is a sharp drop of the spectrum at 52 GeV and this endpoint is the mass difference ($m_{\tilde{\chi}_2^0} - m_{\tilde{\chi}_1^0}$). The measurement of the end point will be limited by an experimental systematic error of order 50 MeV [20] from the absolute calibration of the electromagneticcalorimeter and not by statistics. The masses of $\tilde{\chi}_2^0$ and $\tilde{\chi}_1^0$ are both proportional to the common gaugino mass. The correlation between mass difference and $m_{1/2}$ for mSUGRA models within the following bounds: $95 < m_{1/2} < 105$ GeV, $195 < m_0 < 205$ GeV, $A = 0, 2 < \tan\beta < 10$ and $\mu < 0$ are displayed in Fig. 8. One can see that a measurement of the neutralino mass difference could be used to determine $m_{1/2}$ precisely. For more details refer to [21].

B. Measurement of the Mass Difference $m_{\tilde{g}} - m_{\tilde{b}_L}$

In the gluino decay chain $\tilde{g} \rightarrow \tilde{b}_L b, \tilde{b}_L \rightarrow \tilde{\chi}_2^0 b, \tilde{\chi}_2^0 \rightarrow \ell^+ \ell^- \tilde{\chi}_1^0$, the momentum of the $\tilde{\chi}_2^0$ can be measured with a partial reconstruction technique after the reconstruction of the decay $\tilde{\chi}_2^0 \rightarrow \ell^+ \ell^- \tilde{\chi}_1^0$, if the $\tilde{\chi}_1^0$ mass is known [22]. Since we do not know $m_{\tilde{\chi}_1^0}$, we have to assume a value for $m_{\tilde{\chi}_1^0}$ to carry through the analysis, and then we have to check that our results do not depend on the value assumed. By selecting events near the end point of the dilepton invariant mass, i. e. between 48.0 and 54.0 GeV for point D, the $\tilde{\chi}_1^0$ and the $\ell^+ \ell^-$ system are almost at rest in the $\tilde{\chi}_2^0$ center of mass system. The momentum of $\tilde{\chi}_2^0$ in the lab frame can then be reconstructed using the relation
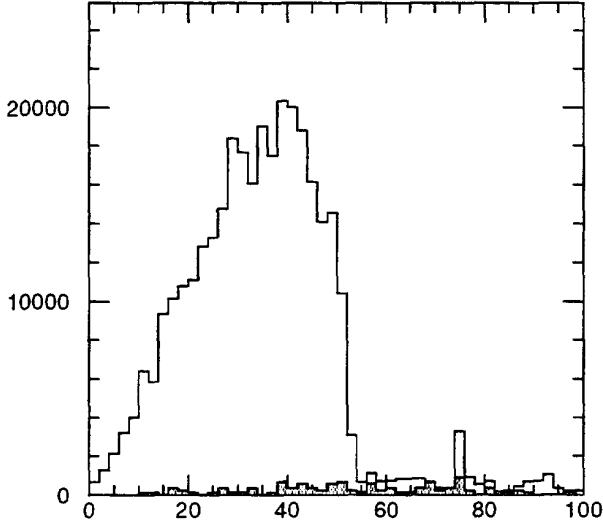
8

like processes. The heavier charginos and neutralinos are only rarely produced in the decays of gluinos, so again their dominant production mechanism is electroweak. The production rate is large. An attempt has been made to isolate these processes. Events are selected that have

- three isolated leptons of which there is a pair of which have opposite charge and the same flavor with $p_{T\ell} > 10$ GeV and $|\eta| < 2.5$;

- No jets with $p_t > 30 GeV$ in $|\eta| < 3.0$.

The jet veto is needed to remove gluino and squark initiated events, which have jets in the central region arising from the decay products of the sparticles and from final state gluon radiation. These events also have jets, approximately uniform in rapidity, from initial state radiation. This latter source is also present in the direct production of chargino, neutralino and slepton production. Figure 12 shows the dilepton invariant mass distribution of the two leptons that have opposite charge and the same flavor. The number of *generated* events in this plot is not large, but are sufficient to demonstrate that in $10\mathrm{fb}^{-1}$ of data there will be sufficient events for a precise measurement. The background events in this plot (corresponding to three generated events) are from $t\bar{t}$ production, the third lepton being from the decay of a $b - quark$. A stricter jet veto (20 GeV instead of 30 GeV) reduces this background further. There is an indication of an edge in the mass distribution corresponding to

Figure 7: The reconstructed dilepton invariant mass in Point D. The signal comes from $\tilde{\chi}_2^0 \rightarrow \tilde{\chi}_1^0 \ell^- \ell^+$ decays. The hatched area is background from $t\bar{t}$.

$$\vec{P}_{\tilde{\chi}_2^0} = (1 + \frac{m_{\tilde{\chi}_1^0}}{M_{\ell^+\ell^-}}) \cdot \vec{P}_{l^+l^-}$$

The mass of $\tilde{b}_L$ is then reconstructed by combining the $\tilde{\chi}_2^0$ with any one of the tagged b jets. The $\tilde{b}_L$ momentum is then combined with one of the other b jet to reconstruct the $\tilde{g}$. One has to take all possible combinations of $\tilde{\chi}_2^0$ and b jets to reconstruct the gluino.

We show in Fig. 9 the scatter plot of $\Delta m = m_{\tilde{g}} - m_{\tilde{b}_L}$ vs $m_{\tilde{b}_L}$. The projections onto the $m_{\tilde{b}_L}$ and Δm axes are shown in Fig. 10 and in Fig. 11, respectively. The mass splitting $\Delta m = m_{\tilde{g}} - m_{\tilde{b}_L}$ is then obtained by fitting the Δm distribution in Fig. 11.

Approximately 6000 gluino and sbottom events can be reconstructed in this channel when running one year at low luminosity . This allows us to measure the mass difference $m_{\tilde{g}} - m_{\tilde{b}_L}$ with good precision. Given the large number of events, the uncertainty of the mass difference will be less than ± 2 GeV. The mass difference turns out to be insensitive to the value for the $\tilde{\chi}_1^0$ mass assumed. For more details we refer to [22].

C. Electroweak Production of Superpartners

At point D sleptons cannot be produced from the decay of strongly interacting sparticles. The production rates are therefore quite small despite the low masses ($m_{\tilde{e}_L} = 215$ GeV, $m_{\tilde{e}_R} = 206$ GeV) as they must be pair produced in Drell-Yan
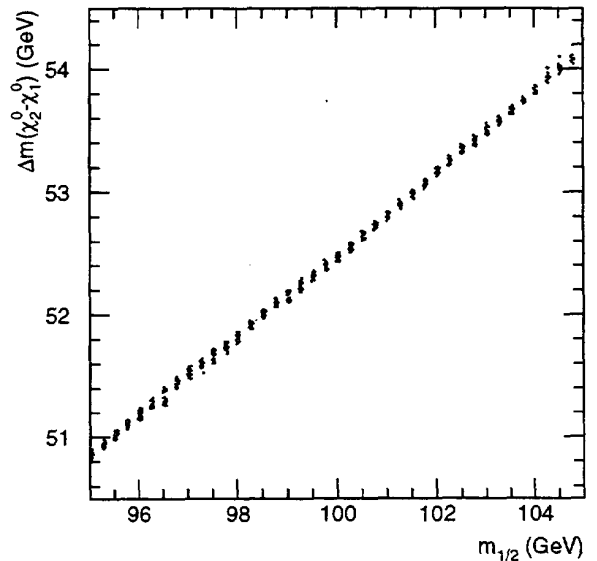
Figure 8: $(m_{\tilde{\chi}_2^0} - m_{\tilde{\chi}_1^0})$ as function of $m_{1/2}$ for mSUGRA models in the range $95 < m_{1/2} < 105$ GeV, $195 < m_0 < 205$ GeV, $A_0 = 0$, $2 < \tan\beta < 10$ and $\mathrm{sgn}(\mu) < 0$
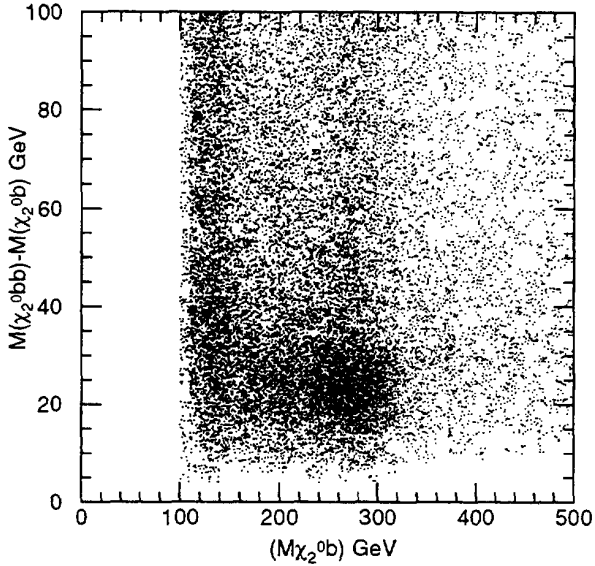
9

Figure 9: Scatter plot of reconstructed $(m_{\tilde{g}} - m_{\tilde{b}_L})$ vs. $m_{\tilde{g}}$ from gluino cascade decay at Point D.
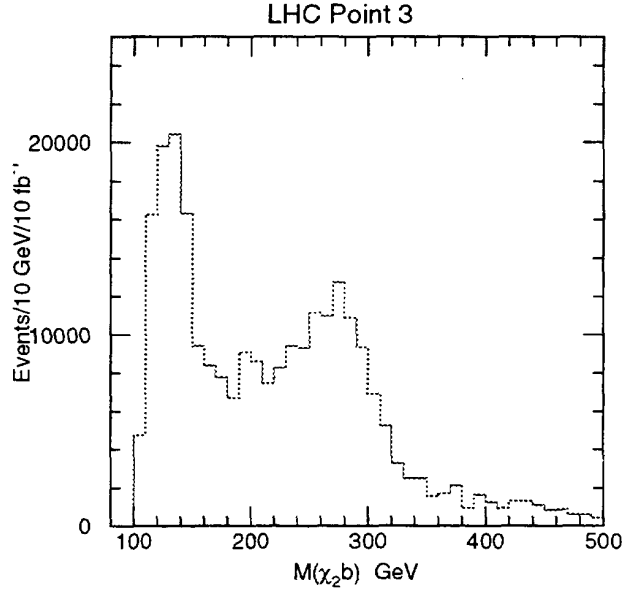
Figure 10: Distribution of reconstructed $m_{\tilde{b}_L}$. This is the x-projection of the scatter plot in Fig. 9.

the decay $\tilde{\chi}_2^0 \rightarrow \tilde{\chi}_1^0 \ell^+ \ell^-$. The events in this plot are dominated by the production of $\tilde{\chi}_2^0 \tilde{\chi}_1^{\pm}$ final states whose contribution is shown as the dotted histogram. If two isolated leptons are required and the same plot made, the result is more events. There is now a potential background from Drell-Yan production of dilepton events which must be eliminated by a cut on missing transverse energy or the angle between the two leptons; the Drell-Yan events are back to back while in the SUSY events the leptons arise from $\tilde{\chi}_2^0 \rightarrow \tilde{\chi}_1^0 \ell^+ \ell^-$ and are therefore close in angle. The production rates in these two and three lepton channels can be compared and used to provide a powerful argument concerning the origin of the lepton samples and provide an additional constraint on the model since, as we will demonstrate in section X, the measurement that have been made using the strong production of sparticles fix the model parameters, resulting in a **prediction** for the rates shown in Figures 12. In principle, the decay $\tilde{\ell}_L \rightarrow \tilde{\chi}_2^0 \ell$ should be reconstructible by selecting with a least 3 isolated leptons, an oppositely charged pair of which have mass between 45 and 55 GeV. The momentum of $\tilde{\chi}_2^0$ is reconstructed as above and then combined with a third lepton to search for a reconstructed $\tilde{\ell}_L$. The extraction of this signal is very difficult. The production rate for gauginos provides a serious background. This background can only be controlled by increasing the number of isolated leptons required. The dominant slepton production process is $\tilde{\ell}_L + \tilde{\nu}$. This can be extracted only by requiring at least **four** isolated leptons from the decay chain $\tilde{\ell}_L(\rightarrow \ell^+ \ell^- \ell \tilde{\chi}_1^0) + \tilde{\nu}(\rightarrow \ell \chi_1^+(\rightarrow \ell \nu \chi_1^0))$ or $\tilde{\ell}_L(\rightarrow \ell^+ \ell^- \ell \chi_1^0) + \tilde{\nu}(\rightarrow \ell \chi_1^+(\rightarrow \ell^+ \ell^- \nu \chi_1^0))$. The dominant

decay chain $\tilde{\nu}(\rightarrow \ell \chi_1^+(\rightarrow jets + \chi_1^0))$ is killed by the jet veto requirement.

D. Tau Polarization in $\tilde{\chi}_2^0$ Decays

In the leptonic decay $\tilde{\chi}_2^0 \rightarrow \tilde{\chi}_1^0 \ell^+ \ell^-$ the leptons in the final state are polarized. In the case that the final-state leptons are $\tau^{\pm}$'s, this polarization can be measured by measuring the decay distributions e: g. in $\tau \rightarrow \pi \nu$, $\tau \rightarrow \rho \nu$ or $\tau \rightarrow a_1 \nu$. This provides complementary information to measurements of the leptonic or hadronic decay branching ratios, the dilepton invariant mass distribution, etc [23].

The decay $\tilde{\chi}_2^0 \rightarrow \tilde{\chi}_1^0 \tau^+ \tau^-$ proceeds via Z^0 exchange and $\tilde{\tau}_i$ exchange, $i = 1, 2$. The Feynman diagrams are shown in Fig. 13 (note that there is a third diagram analogous to diagram a) with τ^+ and τ^- interchanged). In order to describe the basic idea let us assume that either $\tilde{\chi}_2^0$ or $\tilde{\chi}_1^0$ is almost a pure gaugino, and left-right mixing of the $\tilde{\tau}$'s can be neglected. Then diagram b) does not contribute, and in diagram a) the unmixed states $\tilde{\tau}_L$ and $\tilde{\tau}_R$ are exchanged. Then $\tilde{\tau}_L$ couples only to left-polarized τ's and $\tilde{\tau}_R$ only to right-polarized τ's. Furthermore, $\tilde{\tau}_R$ couples only to the $\tilde{B}$ component of $\tilde{\chi}_2^0$ and $\tilde{\chi}_1^0$, whereas $\tilde{\tau}_L$ couples to the $\tilde{B}$ and $\tilde{W}^3$ components. Therefore, the polarization of the final-state τ's contains information about the mixing of the $\tilde{\tau}$'s in the intermediate state and about the mixing of the neutralinos $\tilde{\chi}_2^0$ and $\tilde{\chi}_1^0$. This has been worked out in more detail in [23], where the formulae for the dilepton mass distribution corresponding to diagram a) (and that with τ^+ and τ^- inter-
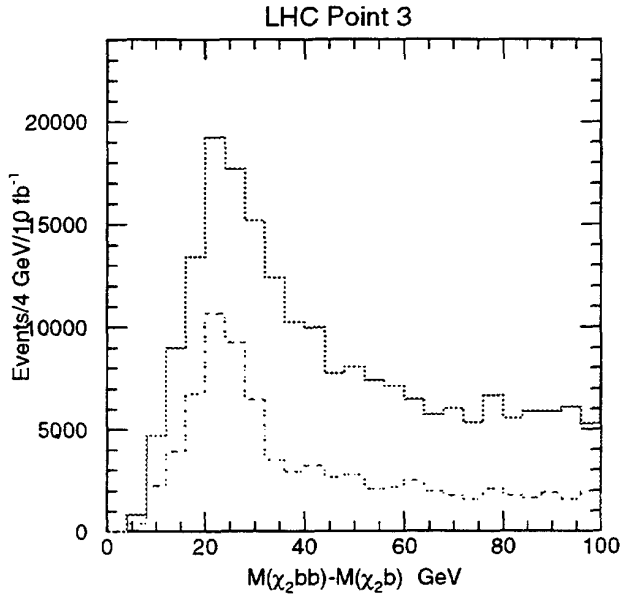
LHC Point 3

LHC Point 3

Figure 11: Distribution of mass difference $(m_{\tilde{g}} - m_{\tilde{b}_L})$. This is the y-projection of the scatter plot in Fig. 9.

changed) for $\tilde{\tau}_L$ and $\tilde{\tau}_R$ exchange are given for the case that the neutralinos are pure $\tilde{B} - \widetilde{W}^3$ mixtures. In this approximation the $\tilde{\chi}_i^0 \tilde{\ell}_R \ell_R$ and $\tilde{\chi}_i^0 \tilde{\ell}_L \ell_L$ couplings are $g_{R_i} \propto \tan \Theta_W \cdot N_{\tilde{B}_i}$ and $g_{L_i} \propto (1/2)(\tan \Theta_W \cdot N_{\tilde{B}_i} + N_{\widetilde{W}^3_i})$, where $N_{\tilde{B}_i}$ and $N_{\widetilde{W}^3_i}$) are the amounts of the $\tilde{B}$ and $\widetilde{W}^3$ components of $\tilde{\chi}_i^0$. The dilepton mass distribution in the $\tilde{\chi}_2^0$ rest frame for left-handed τ^- and right-handed τ^+ due to diagram a) with $\tilde{\tau}_L$ exchange then reads

$$\frac{d\Gamma}{M_{\ell\ell}^2} \propto \left(\frac{2g_{L_1}g_{L_2}}{m_{\tilde{\tau}_L}^2}\right)^2 p_1 \left[(m_{\tilde{\chi}_2^0}^2 - m_{\tilde{\chi}_1^0}^2) E_{\ell\ell} \right.$$

$$\left. -m_{\tilde{\chi}_2^0}(E_{\ell\ell}^2 + \frac{1}{3}p_{\ell\ell}^2) + m_{\tilde{\chi}_1^0} M_{\ell\ell}\right]$$

where $E_{\ell\ell}$ and $p_{\ell\ell}$ are the energy and momentum of the $\tau^+\tau^-$ pair in the $\tilde{\chi}_2^0$ rest frame, $M_{\ell\ell}$ is its invariant mass, and p_1 is the momentum of $\tilde{\chi}_1^0$ in the $\tilde{\chi}_2^0$ rest frame. The result for $\tilde{\tau}_R$ exchange, with the production of a right-handed τ^- and a left-handed τ^+ is obtained by the replacement $g_{L_1}g_{L_2}/m_{\tilde{\tau}_L}^2 \rightarrow g_{R_1}g_{R_2}/m_{\tilde{\tau}_R}^2$.

The polarization of the τ^+ and τ^- is reflected in their decay distributions. For example, for $\tau^- \rightarrow \pi^- \nu_\tau$, the energy distribution of the π^- is
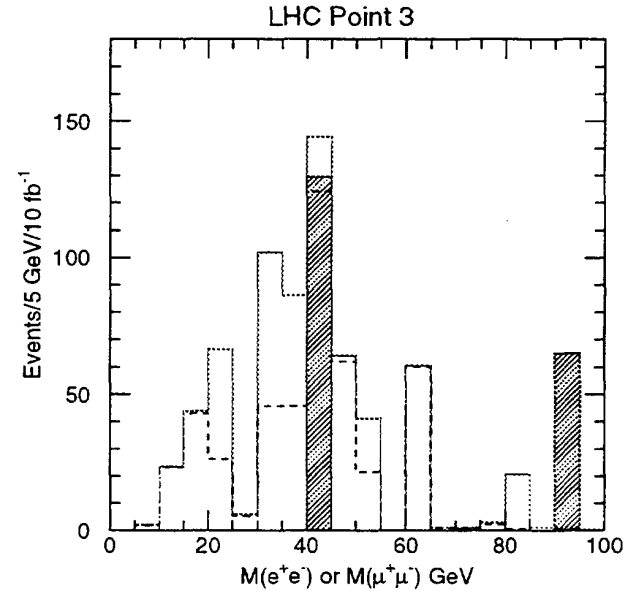
$$\frac{dN}{dx} = 2(1 - x)$$

Figure 12: The invariant mass distribution of e^+e^- and $\mu^+\mu^-$ pairs arising at Point D. Events are selected requiring no jets with $p_t > 30 \text{ GeV}$ in $|\eta| < 3$ and at least three isolated leptons, two of which are of the same flavor and opposite charge. The dashed histogram shows the contribution arising from $\chi_1^+\chi_2^0$ final states. The background is shown as the hatched histogram.

for left-handed τ^-, and

$$\frac{dN}{dx} = 2x$$

for right-handed τ^-, where x is the ratio of the π^- and τ^- energies. In order to obtain the invariant mass distribution of the observed $\pi^+\pi^-$ pair, the expression for $d\Gamma/M_{\ell\ell}^2$ has to be folded with the appropriate τ decay distributions. As shown in [23], in the limiting case considered the two possible τ polarization states, $\tau_L^+\tau_R^-$ and $\tau_R^+\tau_L^-$, lead to distinguishable $\pi^+\pi^-$ mass distributions. Of course, in the general case of neutralino mixing also diagram b) will contribute and will influence the τ polarization. For $\tan \beta \gtrsim 20$ also the Yukawa coupling of the $\tilde{\tau}$'s to the higgsino components of the $\tilde{\chi}_{1,2}^0$ has to be taken into account. In this case also $\tilde{\tau}_L - \tilde{\tau}_R$ mixing has to be included, i. e. in diagram a) the mass eigenstates $\tilde{\tau}_i, i = 1, 2$ will be exchanged. If information on neutralino mixing can be obtained from other experimental data, e. g. from a measurement of the leptonic and hadronic branching ratios of the $\tilde{\chi}_2^0$, then a measurement of the τ polarization can give important information on the mixing of the $\tilde{\tau}$'s.

E. Summary of measurements in Point D

In Point D the huge SUSY production allows that measurements performed reach a very high precision. The following
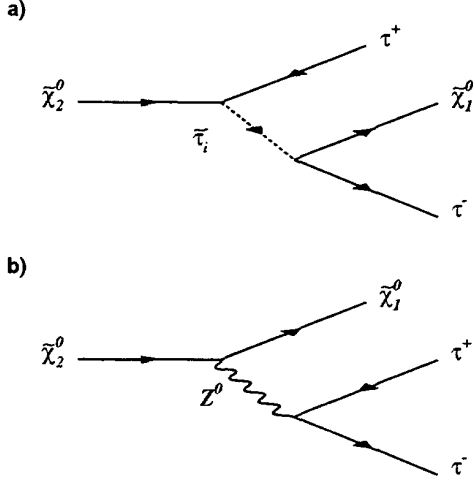
11

a)

τ^+

$\tilde{\chi}_2^0$ $\tilde{\chi}_1^0$

$\tilde{\tau}_i$

τ^-

b)

$\tilde{\chi}_1^0$

$\tilde{\chi}_2^0$ τ^+

Z^0

τ^-

Figure 13: Feynman diagrams for the decay $\tilde{\chi}_2^0 \to \tilde{\chi}_1^0 \tau^+ \tau^-$, a) $\tilde{\tau}_i$ exchange, $i = 1, 2$, and b) Z^0 exchange

quantities are measured with the uncertainty given:

- $m_{\tilde{\chi}_2^0} - m_{\tilde{\chi}_1^0} = 52.36 \pm 0.05$ GeV
- $m_{\tilde{g}} - m_{\tilde{b}_L} = 20.3 \pm 2$ GeV
- m_{h^0} = 68.3 ± 3 GeV (known from LEP2, the error is theoretical)

As is shown in section X these are sufficient to constrain the mSUGRA model. Many more analysis can be done if more statistics is used (here only one year of datataking at low luminosity is considered). Other observables such as electroweak production, branching ratios, tau polarization, slepton production other mass differences give also signals but with less precision, but provide powerful checks of the consistency of a proposed mSUGRA model.

IX. STEP 2: SUSY SEARCHES WITHIN OTHER MODELS

In SUSY models where particles are predicted to be heavier than in point D, the light Higgs boson is too heavy to be discovered before the start of LHC. In many of the "heavy" models the reconstruction of the light Higgs boson mass may be used as a first handle for restricting the model parameters. In parts of the parameter space where $\tilde{\chi}_2^0$ are kinematically allowed to decay in the lightest higgs boson $\tilde{\chi}_2^0 \to h^0 \tilde{\chi}_1^0$ the h^0 production is large. Its mass can be reconstructed from $h^0 \to b\bar{b}$ decays, which also is the dominant $\tilde{\chi}_2^0$ decay mode. From this one learns that $m_{\tilde{\chi}_2^0} - m_{\tilde{\chi}_1^0} > m_{h^0}$. The measurement of the higgs boson

mass and the limit on the neutralino mass difference is a first handle to limit the allowed parameter space and thus searches for more complicated signatures are simplified. The first obvious SUSY signal is however an excess of events with large missing transverse energy. In this section a few examples of reconstruction techniques are given that can be used in SUSY analysis for points A and B.

A. Search for $h^0 \to b\bar{b}$ in SUSY Cascade Decays

As an example $h^0 \to b\bar{b}$ is searched for in point B [24] and in Point A [19]. In point B the fraction of events with $h^0 \to b\bar{b}$ is 30%, being dominated (90%) by single Higgs production. The events were generated with the SPYTHIA Monte Carlo generator [25]. The essential cuts used to extract a clean higgs signal from gluino and squark cascade decays over SUSY combinatorial and SM background are

- $E_T^{miss} > 300$ GeV
- 2 tagged b-jets $p_T^{b-jet} > 50$ GeV
- veto on third tagged b-jet $p_{T,veto}^{b-jet} > 15$ GeV
- veto for isolated lepton $p_T^{lep} > 10$ GeV
- at least 2 extra jets with $p_T^{jet} > 100$ GeV

The invariant mass of the two b-jets shown in Fig. 14 reconstructs well the light Higgs boson mass. The expected precision on the mass measurement is ±1 GeV which is smaller than the theoretical uncertainty. The same decay is present in Point A and the reconstruction of m_{h^0} which is 100 GeV works equally well.

B. Search for $\tilde{\chi}_2^0 \to \ell^\pm \ell^\mp$

In Point A light sleptons contribute to gaugino decays in the channel

$$\tilde{\chi}_2^0 \to \tilde{\ell}_R \ell \to \tilde{\chi}_1^0 \ell^+ \ell^-,$$

which is open and competes with $\tilde{\chi}_2^0 \to \tilde{\chi}_1^0 h^0$, producing opposite-sign, like-flavor dileptons.

The largest SM background is $t\bar{t}$. To suppress this and other SM backgrounds the significant cuts used are:

- $M_{eff} > 800$ GeV
- ≥ 1 jet with $p_{T,1} > 100$ GeV
- $\ell^+ \ell^-$ pair with $p_{T,\ell} > 10$ GeV, $\eta_\ell < 2.5$
- ℓ isolation cut: $E_T < 10$ GeV in $R = 0.2$
- Transverse sphericity $S_T > 0.2$

Because the signal has both a larger color factor and a much larger branching ratio into dileptons than the $t\bar{t}$ background, these cuts produce a dilepton mass distribution, Fig. 15, with very little SM background. This distribution has a sharp edge at the kinematic limit for the two two-body decays,

$$M_{\ell\ell}^{max} = m_{\tilde{\chi}_2^0} \sqrt{1 - \frac{m_{\tilde{\ell}}^2}{m_{\tilde{\chi}_2^0}^2}} \sqrt{1 - \frac{m_{\tilde{\chi}_1^0}^2}{m_{\tilde{\ell}}^2}} \approx 112 \text{ GeV}.$$
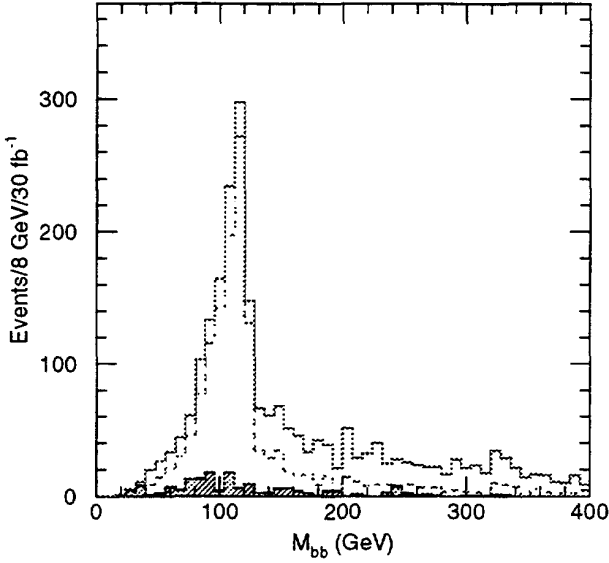
Figure 14: Reconstructed mass of light higgs boson from $h^0 \to b\bar{b}$ decays. Solid line is signal including all backgrounds, the dotted line is $h^0 \to b\bar{b}$ reconstructed without combinatorial background and the hatched area is standard model background.

Figure 15: $M_{\ell\ell}$ distribution for the Point A signal (open histogram) and the sum of all backgrounds (shaded histogram).

Thus, this combination of masses is determined with great precision. Note that $M_{\ell\ell}^{\mathrm{max}}$ vanishes if the phase space vanishes either for $\tilde{\chi}_2^0 \to \tilde{\ell}_R^\pm$ or for $\tilde{\ell}_R \to \tilde{\chi}_1^0 \ell$. The ratio of these decays to $\tilde{\chi}_2^0 \to \tilde{\chi}_1^0 h^0$ contains information on the masses and gaugino mixings. For more details on this analysis refer to [19].

C. Charge and flavour asymmetries

In addition to the mass determination schemes listed here, there exist other variables which can help probe masses and SUSY parameters. Some of these include[17, 4, 2]: charge asymmetries in 1ℓ and SS dilepton events, and flavor asymmetries in OS dilepton events. The former occur because LHC is a pp rather than $p\bar{p}$ collider, so that up and down type squarks are produced preferentially over there anti-matter counterparts. The dilepton flavor asymmetry mainly occurs due to two different major sources for dilepton events: chargino pairs produced in cascade decays lead to ee, $e\mu$ and $\mu\mu$ events, whereas $\tilde{\chi}_2^0$ production in cascade decays leads only to ee or $\mu\mu$ events.

X. STEP 3: CONSTRAINING CANDIDATE SUSY MODELS

The ultimate goal of the SUSY analysis is to combine all measurements into a global fit of candidate SUSY models in a similar way as was done for the LEP data. A global fit is beyond
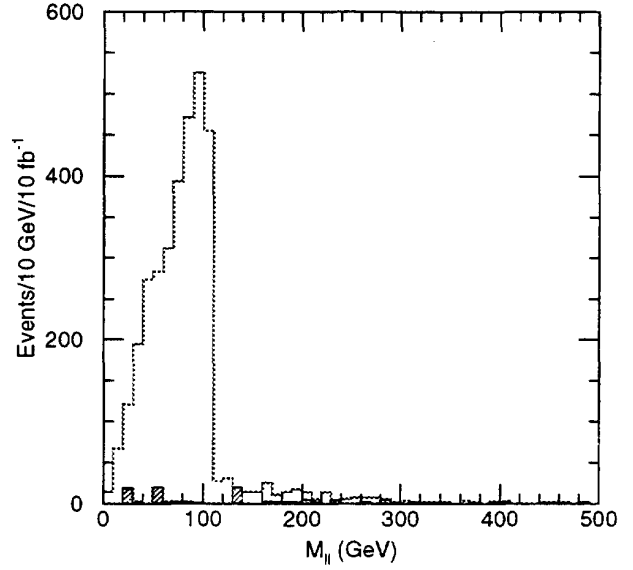
the scope of Snowmass; instead we tried the following. Points were generated randomly in the SUGRA parameter space and then checked if they were consistent with the measurements described in VIII. The constraints on the measured quantities for point D used are

- $m_{\tilde{\chi}_2^0} - m_{\tilde{\chi}_1^0}$ $= 52.36 \pm 0.05$ GeV (1σ)
- $m_{\tilde{g}} - m_{\tilde{b}_L}$ $= 20.3 \pm 2$ GeV (1σ)
- m_{h^0} $= 68 \pm 3$ GeV

The observables and the errors depend on the position in the parameter space. The uncertainty on the parameters from the spread in the models consistent with the constraints above are

- $m_{1/2}$ $= 99.9 \pm 0.7$ GeV
- m_0 $= 200^{+13}_{-8}$ GeV
- $\tan\beta$ $= 1.95 \pm 0.05$
- $\mathrm{sgn}(\mu)$ determined

For the possible candidate models one observation is that the branching ratio $\mathrm{BR}(\tilde{\chi}_2^0 \to \tilde{\chi}_1^0 \ell^- \ell^+)$ varied in the range 14 to 20 %. A measurement of this branching ratio will further constrain the models. The expected accuracy for determination of branching ratios for leptonic decays is ± 1 %. The same random scan method has been tried also to constrain model parameters with measurements from the other LHC SUSY points and worked well also for them.
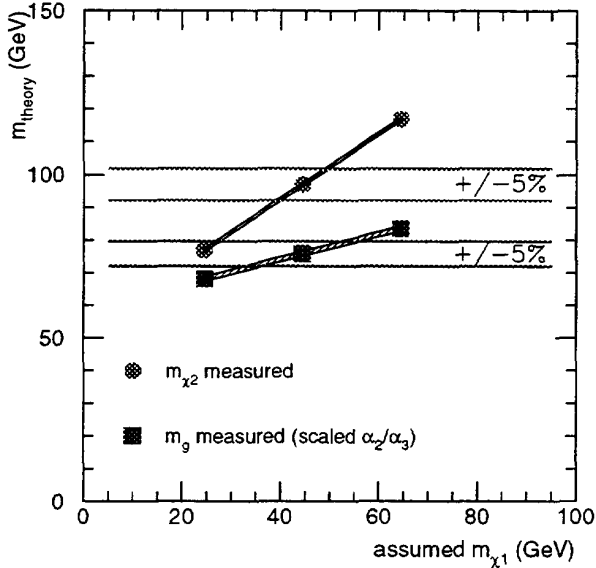
Figure 16: Measured masses (in Point D) as a function of the assumed $\tilde{\chi}_1^0$ mass compared with theoretical predictions.

XI. TEST OF UNIFICATION

We attempted to use the information from measurements in section VIII to test the unification of the gaugino masses. The following procedure was used. The coupling constants α_1, α_2 and α_3 of the $SU(3) \times SU(2) \times U(1)$ are assumed to be measured at low energy. They are extrapolated to find the unification scale M_{GUT}. The observed value of $m_{\tilde{\chi}_2^0} - m_{\tilde{\chi}_1^0}$ is then extrapolated to the GUT scale and used to infer the value of $m_{1/2}$ assuming that they are gaugino like. The masses of the gluino and $\tilde{\chi}_2^0$ are then calculated at the electroweak scale. We assume a 5% theoretical error in this calculation. These values are shown as bands on Figure 16. Also shown on this plot are the values of $m_{\tilde{g}}$ and $m_{\tilde{\chi}_2^0}$ inferred from measurements. These values depend on the assumed value of $m_{\tilde{\chi}_1^0}$ and are shown as a function of that assumed value. There is only one value of $m_{\tilde{\chi}_1^0}$ where the theoretical and "experimental" values of $m_{\tilde{g}}$ agree. This value is used to fix $m_{\tilde{\chi}_1^0}$. The fact that at this same value of $m_{\tilde{\chi}_1^0}$, the theoretical and "experimental" values of $m_{\tilde{\chi}_2^0}$ agree verifies that there is unification of the gaugino masses.

XII. CONCLUSIONS

At LHC there will be an enormous potential for discovering supersymmetry in all of the theoretically favoured parameter space – this includes sparticle masses above 2 TeV, in some scenarios. If weak scale supersymmetry is a correct theory the LHC experiments will not only discover it – they will also make precision measurements. In this report, several examples of pos-

sible starting points for analyses based on simulations of LHC experiments have been given. Inclusive selections are used to determine the supersymmetric mass scale. Determination of individual sparticle masses are possible using partial reconstruction techniques or the invariant mass end-point in three body decays. Furthermore, the production rates and branching fractions of specific supersymmetric processes can be used to evaluate candidate supersymmetric models. In this report, the mSUGRA model is used to illustrate how well LHC experiments can constrain the global parameters of the model. The possibility to perform powerful over-constrained fits (à la the LEP experiments) are also discussed.

In conclusion, the techniques discussed in this report allow an impressive evaluation of a wide variety of candidate supersymmetric models at LHC energies.

XIII. ACKNOWLEDGEMENT

XIV. REFERENCES

[1] L. Ibanez, Phys. Lett. 118B, 73 (1982); J.Ellis, D.V. Nanopolous and K. Tamvakis, Phys. Lett. 121B, 123 (1983); K. Inoue et al. Prog. Theor. Phys. 68, 927 (1982); J. Polchinski and M.B. Wise, Nucl. Phys. B221, 495 (1983); H. P. Nilles, Phys. Rep. 110 (1984) 1; H. E. Haber, G. L. Kane, Phys. Rep. 117 (1985) 75; R. Arnowitt, P. Nath, in Particles and Fields, Proc. of the VII J. A. Swieca Summer School, Sao Paolo, Brazil, 1993, ed. O. Eboli, V. Rivelles (World Scientific, Singapore, 1993); V. Barger, R. J. N. Phillips, in Recent Advances in the Superworld, Proc. of the International Workshop, Woodlands, Texas, 1993, ed. J. Lopez, D. Nanopoulos (World Scientific, Singapore, 1994); Properties of SUSY Particles, ed. L. Ciffarelli, V. Khoze (World Scientific, Singapore, 1993); X. Tata, Lectures presented at TASI95, Univ. of Colorado, Boulder, 1995, hep-ph/9510287

[2] ATLAS Collaboration, Technical Proposal, LHCC/P2 (1994)

[3] CMS Collaboration, Technical Proposal, LHCC/P1 (1994)

[4] H. Baer, C.-H. Chen, F. Paige, X. Tata, Phys. Rev. D 52 (1995) 2746; Phys. Rev. D 53 (1996) 6241

[5] I. Hinchliffe, J. Womersley, LBNL-38997

[6] J. Ellis, et al. Nucl. Phys. B238, 453 (1984); A. Gabutti et. al. hep-ph/9602432; H. Baer, M. Brhlik, Phys. Rev. D 53 (1996) 597

[7] I. Gavrilenko, S Haywood, A.G. Clark, D. Froidevaux and L. Rossi ATLAS internal note, INDET-No-115 (1995)

[8] J. Amundsen et al., these Proceedings

[9] F. Paige and S. Protopopescu, in Supercollider Physics, p. 41, ed. D. Soper (World Scientific, Singapore, 1986); H. Baer, F.

Paige, S. Protopopescu and X. Tata, in *Proceedings of the Workshop on Physics at Current Accelerators and Supercolliders*, ed. J. Hewett, A. White and D. Zeppenfeld, (Argonne National Laboratory, 1993).

[10] R. Barbieri and G. C. Giudice, Nucl. Phys. B 306 (1988) 63

[11] G. Anderson and D. Castaño, Phys. Rev. D 52 (1995) 1693

[12] Contributions of the *Supersymmetry* Working Group, Conveners: G. G. Ross and F. Zwirner, *Proc. of the Large Hadron Collider Workshop*, Aachen, 1990, CERN 90-10, ECFA 90-133, Vol. 2, p. 605, eds.: G. Jarlskog and D. Rein

[13] H. Baer, C. H. Chen, F. Paige and X. Tata, Phys. Rev. D50, 4508 (1994).

[14] H. Baer, C. H. Chen, F. Paige and X. Tata, Phys. Rev, D49, 3283 (1994).

[15] U. Dydak, CMS-TN/96-022 (1996); Diploma Thesis University of Vienna, May 1996

[16] H. Baer, V. Barger, D. Karatas and X. Tata, Phys. Rev. D 36 (1987) 96; R. M. Barnett, J. F. Gunion and H. E. Haber, Phys. Rev. Lett. 60 (1988) 401; Phys. Rev. D 37 (1988) 1892; A. Bartl, W. Majerotto, B. Mösslacher, N. Oshimo and S. Stippel, Phys. Rev. D 43 (1991) 2214; A. Bartl, W. Majerotto and W. Porod, Z. Phys. C 64 (1994) 499

[17] H. Baer, M. Drees, C. Kao, M. Nojiri and X. Tata, Phys. Rev. D50, 2148 (1994).

[18] H. Baer, C. H. Chen and X. Tata, hep-ph/9608221.

[19] F. E. Paige, these Proceedings

[20] F. Gianotti, CERN and L. Serin, LAL Orsay, private communication.

[21] J. Söderqvist, these Proceedings

[22] W. Yao, these Proceedings

[23] R. N. Cahn, these Proceedings

[24] E. Richter-Was, D. Froidevaux, ATLAS SUSY meeting June 1996

[25] S. Mrenna, hep-ph/9609360 (1996)